THE JOURNAL OF BIOLOGICAL CHEMISTRY
Vol. 279, No. 35, Issue of August 27, pp. 37061–37068, 2004
Printed in U.S.A.
© 2004 by The American Society for Biochemistry and Molecular Biology, Inc.

Proteomic Characterization of Postmortem Amyloid Plaques Isolated by Laser Capture Microdissection*[S]

Received for publication, April 2, 2004, and in revised form, June 24, 2004
Published, JBC Papers in Press, June 25, 2004, DOI 10.1074/jbc.M403672200

Lujian Liao‡§, Dongmei Cheng‡§, Jian Wang‡§, Duc M. Duong‡§, Tatyana G. Losik‡§, Marla Gearing§¶, Howard D. Rees§‖, James J. Lah§‖, Allan I. Levey§‖, and Junmin Peng‡§**

From the ‡Department of Human Genetics, §Center for Neurodegenerative Disease, the ¶Department of Pathology and Laboratory Medicine, and the ‖Department of Neurology, Emory University School of Medicine, Atlanta, Georgia 30322

The presence of amyloid plaques in the brain is one of the pathological hallmarks of Alzheimer's disease (AD). We report here a comprehensive proteomic analysis of senile plaques from postmortem AD brain tissues. Senile plaques labeled with thioflavin-S were procured by laser capture microdissection, and their protein components were analyzed by liquid chromatography coupled with tandem mass spectrometry. We identified a total of 488 proteins coisolated with the plaques, and we found multiple phosphorylation sites on the neurofilament intermediate chain, implicating the complexity and diversity of cellular processes involved in the plaque formation. More significantly, we identified 26 proteins enriched in the plaques of two AD cases by quantitative comparison with surrounding non-plaque tissues. The localization of several proteins in the plaques was further confirmed by the approach of immunohistochemistry. In addition to previously identified plaque constituents, we discovered novel association of dynein heavy chain with the plaques in human postmortem brain and in a double transgenic AD mouse model, suggesting that neuronal transport may play a role in neuritic degeneration. Overall, our results revealed for the first time the sub-proteome of amyloid plaques that is important for further studies on disease biomarker identification and molecular mechanisms of AD pathogenesis.

Alzheimer's disease (AD)[1] is a devastating neurological disorder that impairs cognitive function and disturbs emotion and personality. Histopathologically, AD is manifested by the extracellular aggregation of amyloid plaques and the intraneuronal neurofibrillary tangles. Although current amyloid cascade hypothesis (1) or tau hypothesis (2) provides a framework for studying AD pathogenesis, the detailed molecular mechanisms that translate amyloid or tau accumulation into neuronal damage and functional brain impairments are largely unknown. In addition, there are numerous, complex pathological changes in AD brain that contribute to neuronal and synaptic degeneration, including mitochondrial dysfunction, oxidative damage, and inflammation (3–5).

The first major breakthrough in understanding the molecular pathogenesis of AD came from the biochemical purification of amyloid β-peptide (Aβ) from senile plaques, as described by Glenner and Wong (6), and the subsequent sequencing and identification of the Aβ precursor protein (APP) gene. Although the major insoluble component of plaques has been identified as Aβ (6, 7), the entire molecular composition of the plaques is not known. The plaques are highly complex structures with a variety of neural and glial elements (8), and many proteins have been localized to these structures by immunohistochemistry. However, biochemical verification of the plaque components has been scarce. Moreover, biochemical approaches previously applied to purify plaque components generally use very stringent extraction conditions (*e.g.* high concentration of salt, urea, and/or protease treatment) that may remove Aβ-associated proteins. The identities and roles of other plaque proteins that may act synergistically or competitively with Aβ in aggregation and deposition are also incomplete. A systematic analysis of plaque proteins should shed light on the underlying molecular processes that govern the plaque formation.

Traditionally, proteomic analysis is performed by comparing samples between AD cases and normal controls in two-dimensional gels and identifying proteins of interest by mass spectrometry (9). Several groups (10, 11) have tried this strategy and identified some proteins that are altered in the expression levels. However, the two-dimensional gel method is generally incompatible with proteins of extreme size, *pI*, and/or hydrophobicity, and it is tedious to determine the identity of hundreds of protein spots displayed on a two-dimensional gel. Many of the limitations can be overcome by the development of liquid chromatography combined with tandem mass spectrometry (LC-MS/MS) (12, 13). It is now possible to analyze hundreds to thousands of proteins directly from a complex protein mixture, and the sensitivity can reach low femtomole and even subfemtomole levels. The power of shotgun LC-MS/MS-based proteomics technology has been documented by successful proteomic analysis of subcellular structures in mammalian cells, such as nucleolus (14), centrosome (15), nuclear envelope (16), mitochondria (17), and postsynaptic density (18). The methodology has also been used to address dynamic changes in protein levels under specific conditions, as exemplified by the identification of protein components in the epidermal growth factor signaling pathway (19) and the functional investigation of the *myc* oncogene (20). Mass spectrometry has also greatly simplified the analysis of post-translational modifications (21, 22).

Whereas it may be problematic to isolate plaques to homogeneity by using traditional biochemical methods, the advent of laser capture microdissection (LCM) allows procuring a microscopic region as small as 3–5 μm in diameter (23). The LCM technology has been used extensively to collect homogeneous cell

* The costs of publication of this article were defrayed in part by the payment of page charges. This article must therefore be hereby marked "*advertisement*" in accordance with 18 U.S.C. Section 1734 solely to indicate this fact.

[S] The on-line version of this article (available at http://www.jbc.org) contains Table S1.

** To whom correspondence should be addressed. E-mail: jpeng@genetics.emory.edu.

[1] The abbreviations used are: AD, Alzheimer's disease; LC-MS/MS, liquid chromatography coupled with tandem mass spectrometry; LCM, laser capture microdissection; Aβ, amyloid β-peptide; APP, Aβ precursor protein.

This is an Open Access article under the CC BY license.

types for DNA mutation detection and gene expression analysis at the mRNA level (23). More recently, its application in proteomics has begun to be appreciated (24, 25). It is possible to use LCM to capture neuropathological structures with high purity, but the amount of samples collected by LCM is often limited, complicating proteomic analysis by two-dimensional gel-based methods. These limitations can be alleviated by the integration of LCM with the highly sensitive LC-MS/MS technology.

Here we present the isolation of postmortem amyloid plaques labeled with thioflavin-S by using the LCM approach and the systematic identification of extracted proteins by LC-MS/MS. The entire procedure was performed twice with samples from two AD cases. Together, more than 480 proteins were detected in the plaque samples, and 26 proteins were shown to be enriched in the plaques in comparison with the surrounding tissue. The presence of selected proteins in the plaques was confirmed by immunohistochemistry, and cytoplasmic dynein was found to be a novel component of amyloid plaques in human specimens and in an AD mouse model. These studies demonstrate a powerful new approach for achieving comprehensive analysis of the sub-proteome of neuropathological structures.

MATERIALS AND METHODS

Brain Sections—Small blocks of fresh frontal and temporal cortex were obtained at autopsy from a 55-year-old Caucasian female (postmortem interval, 4.5 h, case 1) and a 78-year-old Caucasian male (postmortem interval, 17.5 h, case 2). Both cases were neuropathologically diagnosed as definite AD according to CERAD criteria (26). The brain blocks were embedded in Tissue-Tek® OCT Compound (Jed Pella Inc., Redding, CA), frozen on dry ice, and stored at −80 °C. 10-μm-thick brain sections were cut by using a Leica CM 3050 cryostat (Leica Microsystems Inc., Bannockburn, IL) and mounted on uncoated and uncharged glass slides.

Laser Capture Microdissection—Isolation of plaques by LCM was performed based on the protocol developed previously (27). The frozen brain sections were thawed at room temperature, fixed with 75% ethanol for 1 min, stained with 1% thioflavin-S for 1 min, differentiated in 75% ethanol for 1 min, and then subjected to dehydration in a series of graded ethanol. Finally, the slides were cleared in xylene for 5 min and then air-dried and desiccated. LCM was performed the same day under a fluorescence microscope attached to a Pixcell II laser capture facility (Arcturus, Mountain View, CA) with the following settings: excitation wavelength, 495 nm; laser power, 60–80 milliwatts; duration, 1 ms; and laser spot size, 7.5 μm. A total of about 2000 amyloid plaques were procured from four cortical sections in both cases. Non-plaque areas surrounding the plaques were captured as a control. Each CapSure Macro LCM cap (Arcturus, Mountain View, CA) was used for the capture of about 500 plaques or control tissues from one slide.

Protein Extraction and Analysis by Mass Spectrometry—The caps were extracted twice with lysis buffer at 65 °C for 15 min. The lysis buffer was made from phosphate-buffered saline buffer, pH 7.2, with the addition of 2% SDS, 10% glycerol, 10 mM dithiothreitol, 1 mM EDTA, and protease inhibitor mixture (Roche Applied Science). After the extraction, the samples were alkylated with 50 mM iodoacetamide in the dark at room temperature for 30 min. The total amount of proteins in the samples was estimated on a silver-stained SDS gel according to a standard protein marker with known concentration.

For mass spectrometry analysis, proteins in each sample were separated on a 6–12% SDS gel (0.75 mm thick) and stained with Coomassie Blue G-250. The entire lane was cut into 15 pieces followed by in-gel trypsin digestion (28). The resulting peptides from each gel piece were dissolved in buffer A (0.4% acetic acid, 0.005% heptafluorobutyric acid, 5% acetonitrile). A pressure cell was used to load each sample onto a 50-μm inner diameter × 12-cm self-packed, fused silica C18 capillary column as described (29). Peptides were eluted during a 2-h gradient from 10 to 30% buffer B (0.4% acetic acid, 0.005% heptafluorobutyric acid, 95% acetonitrile; flow rate, ~300 nl/min). Eluted peptides were ionized under high voltage (1.8–2 kV) and detected in an MS survey scan from 400 to 1700 atomic mass units with 2 microscans followed by three data-dependent MS/MS scans (3 microscans each, isolation width 3 atomic mass units, 35% normalized collision energy, dynamic range 3 min) in a completely automated fashion on an LCQ-DECA XP-Plus ion trap mass spectrometer (Thermo Finnigan, San Jose, CA).

Database Searching for Protein Identification—The Sequest algorithm (30) was utilized for searching all MS/MS spectra against the human reference data base (ftp.ncbi.nih.gov/genbank, July, 2003). The parameters were set to allow parent ion mass tolerance to be three and to consider only the b and y ion series. Modifications were permitted to allow the detection of the following (mass shift shown in daltons): oxidized methionine (+16), carboxymethylated cysteine (+57), and phosphorylated serine, threonine, and tyrosine (+80). We used more stringent Sequest criteria than described previously (31, 32): 1) only fully tryptic peptides were considered; 2) ΔCn score is at least 0.08; and 3) Xcorr should be larger than 2.0, 1.7, or 3.3 for charge states of +1, +2, +3, respectively. To reduce false-positives further, we manually verified proteins matched by less than three peptides, because no false-positives were found among proteins identified by at least three distinct peptides (32). Therefore, all peptides were accepted with high confidence. The conversion from the identified peptides to proteins was complicated by the presence of different names for the same protein and/or by the sharing of peptides within several proteins (*e.g.* protein paralogs) (33). Thus we manually verified all proteins and removed the redundancy. Typically, we accepted proteins identified by at least one "unique peptide." Obvious contaminants such as trypsin and keratins were removed. Finally we merged the data sets of the plaque samples from two independent experiments.

Protein Quantification by Mass Spectrometry—Quantitative protein comparison between the plaques and the non-plaque control was carried out in two steps. The first step was based on the number of peptides identified for an assigned protein, indicative of protein abundance. We discarded proteins that were identified by more peptides in the control than in the plaques from either AD case. The second step was based on extracted ion current of corresponding peptides in MS survey scans (15, 34, 35). The ratio of peak intensities of selected peptides was measured in the 15 pairs of peptide mixtures that were generated by in-gel digestion of the 15 pairs of gel pieces as shown (Fig. 1). We analyzed each pair of samples in two consecutive LC-MS/MS runs on the same column and found that the quantitative variation was within 2-fold in general by using a trypsin auto-cleavage peptide (VATVSLPR, *m/z* 842.5 for singly charged ion) as internal control. Therefore, we used 2-fold as the threshold for protein enrichment in the plaques. The trypsin auto-cleavage peptide was also used to normalize the measured peptide ratios and to normalize the elution time of selected peptides between the pair of LC-MS/MS analyses. It should be mentioned that, in contrast to the peptide identification that was primarily derived from its MS/MS spectrum (Fig. 3*B*), the peptide quantification relied on the MS survey scan (Fig. 3*A*). An MS survey scan allowed the detection of many peptide ion peaks, of which only the most three predominant were selected for sequencing by MS/MS analysis. However, the other nonsequenced peaks on MS survey scans could be useful for quantification. For example, when a peptide was sequenced by MS/MS analysis in the plaque sample but not sequenced in the control, it is still possible to find and quantify the peptide ion in MS survey scans of the control sample according to its predicted m/z value and adjusted elution time. Otherwise, if the peptide could not be reliably located in the control sample, we estimated that the plaque/control ratio was more than 2-fold. Finally, we accepted proteins that were found to be enriched at least 2-fold in both AD cases.

Immunohistochemistry—Nontransgenic and double transgenic C3/B6 mice expressing the APP695 isoform with the "Swedish" double mutation (APPswe) and PS1ΔEx9, a functional PS1 mutant lacking exon 9 (amino acids 290–319) (36, 37), were used. Animals were anesthetized with isoflurane (Abbott) and decapitated, and brains were removed and fixed in 4% paraformaldehyde for up to 6 h. Sections of cingulate cortex from four patients with autopsy-confirmed AD and two normal controls were used. At autopsy, the brains were fixed with formalin for at least 48 h. Brain blocks were then sectioned (50 μm) with a freezing microtome (Microm, Heidelberg, Germany). The brain sections were cryoprotected in 40% sucrose in phosphate-buffered saline buffer (50 mM phosphate-buffered saline, pH 7.2). Double labeling was performed by using rabbit anti-Aβ (1:200, polyclonal antibody, Chemicon, Temecula, CA) together with one of the following monoclonal antibodies: anti-Hsp70/90 (1:200, Stressgen, Victoria, British Columbia, Canada) or anti-vimentin (1:2000, Roche Applied Science). For Aβ colocalization with rabbit anti-dynein heavy chain (1:200, Santa Cruz Biotechnology Inc., Santa Cruz, CA), a monoclonal antibody against Aβ (4G8, 1:200, Chemicon) was used. After primary antibody incubation overnight at 4 °C, the sections were extensively rinsed and incubated with fluorescein isothiocyanate-conjugated donkey anti-rabbit antibody (1:200, Jackson ImmunoResearch, Bar Harbor, ME) and then with biotinylated goat anti-mouse antibody (1:1000, Vector Laboratories,

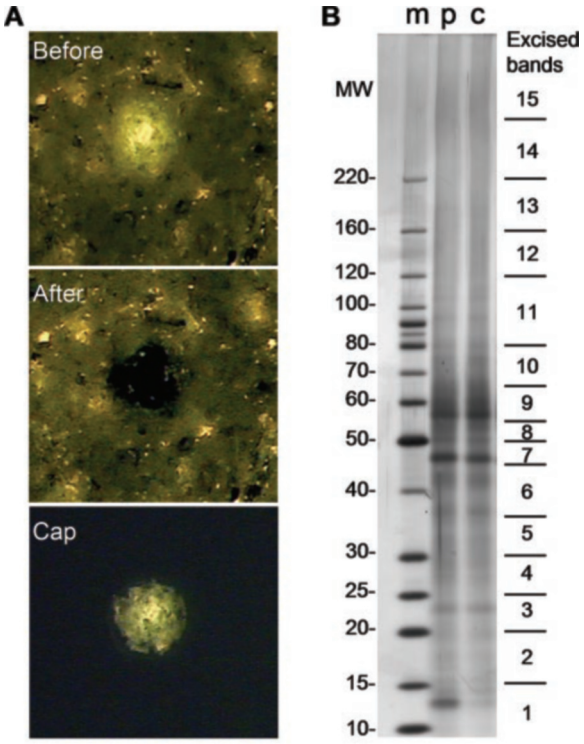

FIG. 1. **Isolation of amyloid plaques by laser capture microdissection.** *A*, the *before* and *after* images indicate the removal of a plaque region from a thioflavin-S-stained AD brain section. The isolated plaque was attached to the cap as shown. Moreover, the surrounding non-plaque regions were also captured as control on a different cap. *B*, protein in the captured plaques (*p*) and non-plaque control (*c*) were extracted by a SDS-containing lysis buffer. A small fraction (~5%) of each sample and molecular weight marker (*m*) was run on an SDS gel followed by silver staining as indicated. The remaining samples (~95%, ~4 μg) were resolved on another SDS gel and stained with Coomassie Blue G-250 (data not shown). Each sample lane was cut into 15 pieces that were subjected to trypsin digestion and LC-MS/MS analysis. The gel excision pattern is shown on the *right* according to the marker.

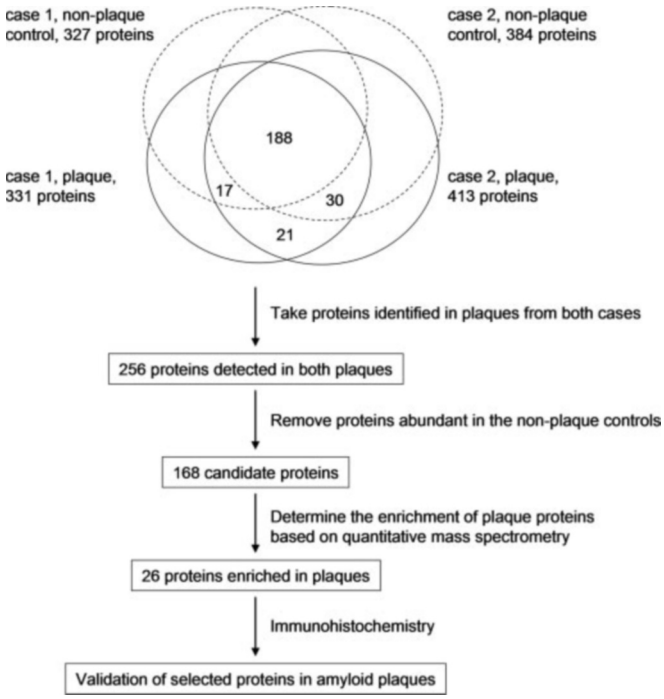

FIG. 2. **Flow chart for the identification of proteins enriched in the plaque regions.** Proteins identified in the plaques and the controls are represented by *solid line circles* and *dashed line circles*, respectively. The number of overlapped proteins in both plaque samples is indicated in the relevant areas. A total of 256 proteins found in both AD plaques was processed in two successive steps: (i) removing proteins that were found to be abundant in the non-plaque control and (ii) quantifying the remaining 168 proteins based on extracted ion current of corresponding peptides. Finally we found that 26 proteins were enriched at least 2-fold in the plaque regions, of which several proteins were further verified by conventional immunohistochemistry.

Burlingame, CA) at room temperature for 2 h. The biotinylated secondary antibody was further detected by avidin-biotin complex and Tyramide Signal Amplification (PerkinElmer Life Sciences). The double-labeled sections were examined with a ×40 objective lens (numeric aperture 1.4) on a LSM510 laser-scanning confocal microscope (Zeiss).

RESULTS

Identification of Proteins Enriched in AD Amyloid Plaques by Quantitative Proteomics—Senile plaques in AD brain tissues were stained with thioflavin-S and isolated by using LCM (Fig. 1*A*). Despite some background staining on the postmortem tissue sections, the plaques were easily distinguishable under the microscope. Approximately 2,000 plaques from one AD brain were captured to yield ~4 μg of total protein after extraction with SDS-containing lysis buffer. The non-plaque regions from the same brain sections were also procured as a control. The total protein samples extracted from the plaques and the non-plaque control were resolved in parallel on an SDS gel (Fig. 1*B*), which indicates a similar protein composition in the two samples. The proteins in the entire gel lanes were analyzed by LC-MS/MS as described under "Materials and Methods." Approximately 30,000 MS/MS spectra were acquired for each sample and searched against a human protein database by using the Sequest program (30). The matched peptides were further filtered rigorously and led to the identification of 331 proteins in the plaques and 327 proteins in the adjacent non-plaque regions of the cortex in this AD case (Fig. 2).

As the plaques are complex and heterogeneous neuropathological structures and are expected to vary among human cases, the protein components may differ in AD patients. We repeated the entire proteomic analysis by using samples isolated from the second AD case and identified 413 proteins in the plaques and 384 proteins in its own non-plaque control (Fig. 2). The data sets from the two AD cases were combined to result in a list of 488 proteins detected in the plaque samples (supplemental Table S1). The current literature identifies about 53 proteins present in the plaques, of which 44 proteins were found in our large scale analyses (Table S1). As expected, many of these proteins were also found in the cortical areas without the plaques, because some normal cellular elements are components of the plaques, including glia and neurons. Alternatively, these proteins may reflect the capture of normal cellular elements along with the plaques.

To determine which of the above proteins were enriched in the plaque regions, we utilized a strategy outlined in Fig. 2. First, only the 256 plaque proteins detected in both AD cases were considered to increase the dataset reliability. Although it is difficult to estimate protein abundance directly from its peptide ion current, the number of peptides identified for each protein is roughly correlated with the abundance of the protein after the protein size is normalized (38, 39). Based on this principle, we removed the proteins that were identified more frequently in the controls than in the plaques according to the corresponding peptide numbers (Fig. 2 and Table S1), and we kept the remaining 168 proteins for further quantitative analysis. More recently, several groups (15, 34, 35) proposed a simple relative quantification method via extracted ion current of peptides in successive analyses. We used this method to quantify the 168 proteins by manual inspection of the raw files. For example, during the LC-MS/MS analysis, an Aβ tryptic

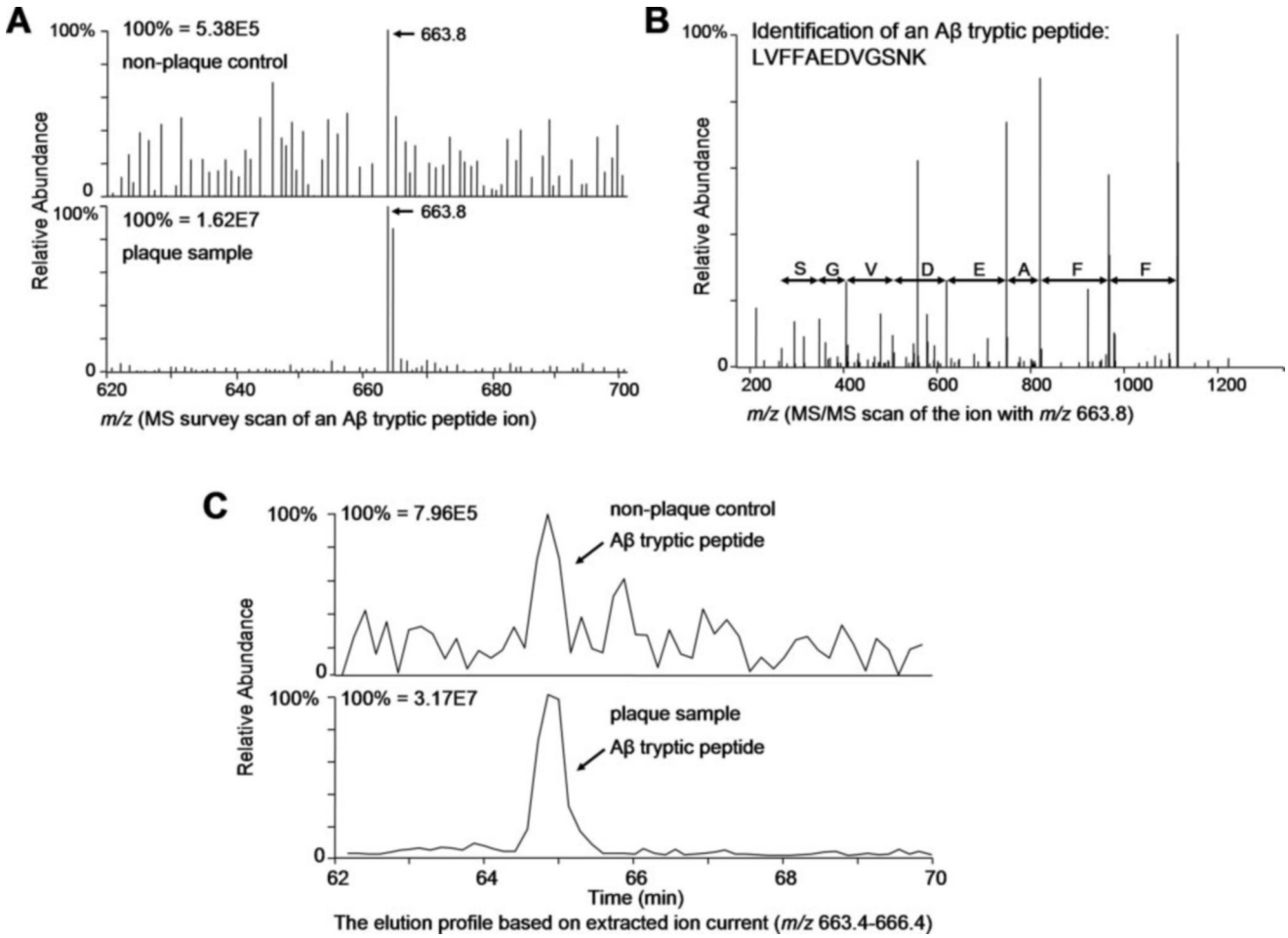

FIG. 3. **Identification and quantification of Aβ by reverse-phase LC-MS/MS.** *A*, comparison of MS survey scans shows that a peptide ion with *m/z* 663.8 is much more abundant in the plaques (*lower panel*) than in the non-plaque control (*upper panel*). A partial region (620–700 *m/z*) is shown for simplicity, although the entire scan range is from 400 to 1700 *m/z*. *B*, MS/MS scan of the precursor ion (663.8 *m/z*), which led to the identification of a tryptic peptide derived from Aβ. *Gaps* between the adjacent product ions fit the mass of amino acid residues as indicated. *C*, the elution profile of the Aβ tryptic peptide (*m/z* 663.4–666.4 due to naturally occurring isotopic distribution) from the non-plaque control and the plaque sample after normalizing the elution time. The peptide was quantified based on the extracted ion current. In fact, the data acquired in LC-MS/MS are three-dimensional (ion current indicated by the relative abundance, retention time of LC, and the *m/z* measurement every ~2 s during the entire LC). *A* was a snapshot of *m/z* measurement at the retention time point of 65 min in *C*.

peptide was detected in an MS survey scan (Fig. 3*A*) and sequenced by MS/MS (Fig. 3*B*) in the plaque sample and the control. The extracted ion current signal for the peptide is shown in Fig. 3*C*, which allows for peptide quantification in both samples. It is worth noting that a trypsin auto-cleavage peptide was used as an internal standard to normalize the experimental variation and to fit the elution time of selected peptides. The plaque/control ratio of Aβ abundance was determined to be around 80, indicative of the enormous enrichment of Aβ in the plaques. The relative abundance of all other proteins was quantified in a similar manner, resulting in the final acceptance of 26 proteins enriched at least 2-fold in the plaques of both AD cases (Table I). However, the majority of previously identified plaque proteins is not on this list because some abundant proteins (*e.g.* actin and tubulin, Table S1) are present but not necessarily concentrated in the plaque, and some low abundance proteins (*e.g.* collagen XXV and antichymotrysin, Table S1) were detected only in one AD case perhaps due to sensitivity limitation of the LC-MS/MS approach. Nevertheless, the list of 26 proteins that were identified and concentrated in the plaque regions in both AD cases are more likely to be genuine plaque proteins.

Classification of Identified Plaque Proteins—To evaluate the proteins identified in the plaques from AD postmortem samples, we grouped them under functional categories in alphabetical order (Table I and Table S1) and discuss the implication of some enriched plaque proteins in AD pathogenesis.

Cell Adhesion and Cytoskeleton and Membrane Trafficking—A number of intercellular adhesion molecules have been shown to be localized in amyloid plaques in AD patients (40). We found that collagen I and fibrinogen were concentrated in the plaques. In addition to extracellular structures, integrity of the intracellular cytoskeleton is important for neuronal physiological functions such as axoplasmic flow of essential synaptic components (41). In our study, all major isoforms of cytoskeletal components, actin, tubulin, and neurofilament, were identified with high numbers of peptides, which indicates that they are abundant species in the plaques as well as in non-plaque regions. Most interestingly, we identified one actin-binding protein, coronin, concentrated in the plaque, although its potential role in pathogenesis remains unclear. Also enriched in plaques is the microtubule-associated protein tau that is more commonly known to be associated with neurofibrillary tangles and neurites (42) and likely represents the dystrophic neurite component in the plaques. The identification of a variety of cytoskeletal protein elements, some of which are known to be relevant to AD, suggests that these elements may be involved in plaque formation, and cytoskeletal impairments may lead to

TABLE I

List of 26 proteins enriched in amyloid plaques as compared with non-plaque areas

The proteins and functional categories were sorted in the alphabetic order. When a peptide in the non-plaque control was not detected, we assumed the ratio was more than 2. Sometimes, even if a peptide ion was not sequenced by MS/MS, it was still possible to identify it in MS survey scan to enable quantification (see "Materials and Methods").

Protein name	GenBank™ accession no.	AD case 1			AD case 2		
		Ctl[a]	Plaque[b]	P/C[c]	Ctl	Plaque	P/C
Cell adhesion							
Collagen I, α-1 polypeptide	NP_000079.1	0	2	3.6	0	1	>2
Fibrinogen, γ	NP_000500.1	0	3	>2	0	2	>2
Channels/receptors							
ATPase, Ca^{2+}-transporting	NP_001674.1	1	3	2.1	0	2	>2
Chaperones							
Heat shock 90-kDa protein 1, β	NP_031381.2	7	9	2.1	11	14	2.0
Cytoskeleton							
Coronin, actin-binding protein	NP_009005.1	0	1	>2	0	1	>2
tau	NP_058519.1	1	3	6.8	2	4	3.2
Inflammation							
Glial fibrillary acidic protein (GFAP)	NP_002046.1	16	21	3.6	20	24	2.1
Vimentin	NP_003371.1	4	12	9	11	15	2.3
Kinases/phosphatases and regulators							
14-3-3 β/α	NP_003395.1	2	4	3.1	5	8	3.5
14-3-3 ϵ	NP_006752.1	2	5	6.1	7	9	4.4
14-3-3 ζ	NP_003397.1	4	6	7.7	5	10	7.4
Membrane trafficking							
Clathrin, heavy polypeptide 1	NP_001826.1	0	1	>2	0	5	2.7
Dynamin 1	NP_004399.1	5	6	2.3	18	23	2.2
Dynein, heavy polypeptide 1	NP_001367.2	0	1	4.8	0	1	>2
Metabolism							
Phosphofructokinase	NP_002618.1	0	2	3.9	3	7	2.5
Others							
Amyloid β-peptide	NP_000475.1	1	1	80.0	0	1	>2
Proteolysis							
Antitrypsin	NP_000286.2	0	3	>2	1	2	2.5
ATPase, H^+-transporting, lysosomal V0 subunit A	NP_005168.2	0	1	>2	1	3	2.4
ATPase, H^+-transporting, lysosomal V1 subunit B	NP_001684.2	0	4	2.1	4	8	3.0
ATPase, H^+-transporting, lysosomal V1 subunit D	NP_057078.1	0	1	>2	1	3	2.6
ATPase, H^+-transporting, lysosomal V1 subunit E	NP_001687.1	1	2	5.0	4	5	8.3
Cathepsin D	NP_001900.1	0	1	>2	0	3	>2
Cystatin B	NP_000091.1	1	2	2.9	0	1	>2
Cystatin C	NP_000090.1	0	1	>2	0	1	>2
Ubiquitin-activating enzyme E1	NP_695012.1	0	1	7.1	3	4	2.0
Vacuolar ATPase subunit H	NP_057025.1	0	1	>2	1	3	2.1

[a] Ctl indicates the number of different peptides that identify a protein in the control samples of non-plaque regions.
[b] Plaque indicates the number of peptides that identify a protein in the plaque samples.
[c] P/C indicates the abundance ratio of proteins from the plaque samples *versus* non-plaque regions.

a deficit in axoplasmic flow and eventually to neuritic dystrophy. Indeed, numerous proteins involved in membrane trafficking and protein sorting were revealed to be concentrated in the plaques by the mass spectrometry analysis, such as clathrin heavy chain, dynamin, and dynein heavy chain (Table I). This observation implicates that the AD plaque might sequester some key proteins to perturb the protein sorting system that is crucial for maintaining normal synaptic plasticity.

Chaperones and Inflammation—It is well known that the senile plaque core is surrounded by activated astrocytes, microglia, and dystrophic neurites (43, 44), and the heat shock proteins exhibit high expression levels in reactive astrocytes in areas rich in senile plaques (45). Consistently, we identified many heat shock proteins (Table S1) and found that HSP90 was enriched in the plaques (Table I). We also identified glial fibrillary acidic protein and vimentin with high numbers of peptides; both are the major components of intermediate filaments in activated glial cells.

Kinase/Phosphatase and Regulators—The imbalance of phosphorylation/dephosphorylation activity is believed to contribute to AD pathology, as evidenced by tau hyperphosphorylation in the neurofibrillary tangles. We identified multiple kinases (Table S1), but none of them were specifically enriched in the plaque regions. Instead, three 14-3-3 isoforms showed a significant degree of enrichment in the isolated plaques. Previous studies have demonstrated that 14-3-3 proteins are present in neurofibrillary tangles (46), and at least one 14-3-3 protein has further been shown to be an effector of tau phosphorylation (47). Moreover, we attempted to detect protein phosphorylation sites in the plaque samples by tandem mass spectrometry, and we located two phosphorylated amino acid residues in neurofilament 3 (SPVPK**S**PVEEK and KAE**S**PVKEEAVAEVVTITK with modified sites shown in boldface with underline). The first phosphorylation site was documented in tandem repeats in the neurofilament sequence and was excessively modified in the AD brain (48). The second peptide indicated a phosphorylation site on serine 736 that we show for the first time. These phosphorylation events may play a role in the formation of dystrophic neurites surrounding the plaque core.

Proteolysis—The ubiquitin-proteasome system plays a crucial role in the degradation of misfolded proteins and turnover of cell signaling molecules (49). This study identified the ubiquitin-activating enzyme enriched in the plaques. More strikingly, numerous subunits of lysosomal ATPase and cathepsin D were found to be concentrated in the plaques, suggesting the high proteolytic activity in the plaques *versus* non-plaque regions. Moreover, we found in the plaques antitrypsin, cystatin B, and cystatin C. Cystatin C is a cysteine proteinase inhibitor and has been shown to be up-regulated in AD and coaggregated with Aβ (50, 51). Cystatin C is also proposed as a potential risk factor for late-onset AD (52). Overall, the relative abundance of proteolytic enzymes and inhibitors in multiple cellular proteo-

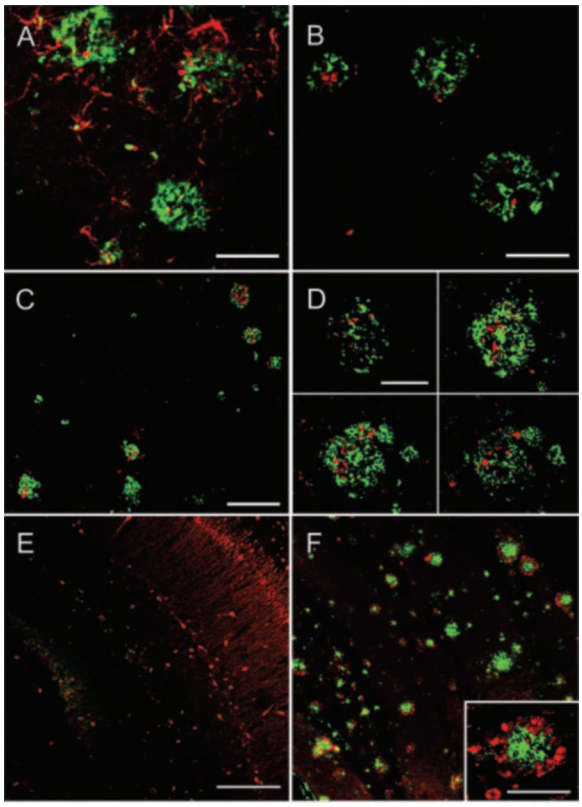

FIG. 4. **Localization of plaque proteins by immunofluorescence confocal microscopy.** Sections of human postmortem AD neocortex were stained with Aβ antibody (either polyclonal anti-Aβ_{40}, *A* and *B*, or monoclonal antibody 4G8, *C* and *D*, *green*) and antibodies against vimentin (*A*, *red*), Hsp70/90 complex (*B*, *red*), or dynein heavy chain (*C* and *D*, *red*). Four serial confocal slices through a plaque region are shown in *D* at a 1-μm optical slice thickness and 4-μm intervals between slices. Brain sections containing cortex and hippocampus from nontransgenic (*E*) and PS1/APP double transgenic mice (*F*) at 9 months of age were labeled with monoclonal Aβ antibody 4G8 (*green*) and polyclonal heavy chain antibodies (*red*). *Scale bar*, *A*, *B*, *D*, and the *insert* in *F*, 50 μm; *C*, *E*, and *F*, 100 μm.

lytic pathways strongly suggests the activation of protein degradation mechanisms and the interplay between proteolysis and inhibition activities during the plaque formation.

Validation of Selected Plaque Components—To verify further the localization of some of the proteins identified, we undertook immunostaining analysis on postmortem brain tissues for their colocalization with Aβ. In Fig. 4*A*, monoclonal antibody against vimentin specifically labeled activated astrocytes surrounding the fibrillary plaque core that was recognized by Aβ antibody, and some astrocyte processes were extended deeply into the plaque core, indicating a local inflammatory response in the plaque region (53, 54). Polyclonal antibodies against the Hsp70 and Hsp90 complex show strong immunoreactive signals in dot-like structure located in the plaque regions (Fig. 4*B*), consistent with our proteomic analysis. More strikingly, dynein heavy chain was detected as punctate and thread-like structures in many plaques labeled by Aβ antibody (Fig. 4*C*), suggesting that dynein heavy chain is a constituent of plaque neurites. Confocal microscopic images clearly indicated that dynein heavy chain was enriched in the plaque, compared with the surrounding neuropil (Fig. 4*D*).

The colocalization of dynein with amyloid plaque was corroborated in an AD model, PS1/APP double transgenic mice (36, 37). As expected, no plaque was visualized in 9-month-old control animals, and dynein heavy chain antibodies labeled the soma and neurites in the cortex and hippocampus (Fig. 4*E*). In great contrast, the similar brain regions in 9-month-old AD mice manifested high density of amyloid plaques, the majority of which is clearly surrounded by dynein immunoreactive structures that may represent enlarged neurites (Fig. 4*F*). Recently, missense mutations in dynein heavy chain have been genetically linked to progressive motor neuron degeneration and the formation of Lewy body-like inclusions (55). It has also been observed previously (56) that dynein immunoreactivity in AD brain tissue is significantly increased compared with normal brain. Given that dynein is responsible for retrograde transport of vesicles along microtubules in the axon (57), the enrichment of dynein encircling the plaque core might trigger trafficking malfunction to cause neuritic dystrophy.

DISCUSSION

Our studies revealed a total of 488 proteins in amyloid plaques, representing three histopathological components: the plaque core, activated glial cells, and dystrophic neurites. Identified intracellular proteins are likely derived from neurites and/or glial cells surrounding the plaque core, whereas extracellular proteins may be components of the plaque core. It is also possible that some intracellular proteins can leak out after plasma membrane damage during neuronal degeneration. By quantitative mass spectrometry, we further identified 26 proteins enriched in the plaques when comparing with the non-plaque control sample from the same AD case. This comparison is particularly valuable because both samples were derived from the same postmortem tissue specimen, which essentially eliminates the effects of many confounding factors (*e.g.* genetic variation, postmortem interval, etc.) that are often encountered in human tissue studies.

Our results confirmed the presence of most proteins that were detected previously in the plaques mainly by immunohistochemistry (40). The classic plaque components identified in this study include Aβ, α1-antichymotrypsin (58), apolipoprotein E (59), collagen type XXV (60), cystatin C (61), α-synuclein (62), proteoglycans (63), and clusterin (64). On the other hand, only a few proteins known to be amyloid plaque components were missed in this study. Those included complement inhibitors (40), myeloperoxidase (5), α_2-macroglobin (65), superoxide dismutase (66), HO-1 (67), catalase (68), and cholinesterase (69). The apparent absence of these proteins in the plaques in our study could be due to the low abundance of the proteins and/or incompatibility of tryptic peptides with the LC-MS/MS system (12). Our results from two independent studies of AD cases revealed that about two-thirds of the proteins were identified in both cases. The difference between the two data sets may be contributed by the sample variation in the patients and the nature of shotgun proteomics strategy, as only a fraction of peptides was selected and sequenced by mass spectrometry when a complex peptide mixture was analyzed by the LC-MS/MS approach (29).

Immunohistochemistry was employed as an independent approach to confirm the proteomic findings. Eight proteins (in Table I and Table S1) were selected largely based on the availability of the antibodies. Most of them are concentrated by varying degrees in the plaque regions, as exemplified by vimentin, Hsp 70/90 complex, dynein (Fig. 4), α-synuclein, glial fibrillary acidic protein, and synaptophysin (data not shown). Other proteins like actin and tubulin display a broad distribution but are not specifically concentrated in the plaques (data not shown), although actin and tubulin are believed to be plaque components. Therefore, the list of 26 proteins according to quantitative analysis should contain much less false plaque constituents.

Aβ is widely accepted as the major component of the amyloid plaque core; consistently, our mass spectrometry analysis identified Aβ in both plaque and non-plaque control but showed it

to be enriched about 80-fold in the plaques. No other proteins were found to accrue at a similar level, suggesting that Aβ is the sole major protein species in the plaque core. Although Aβ aggregates are resistant to extraction by many reagents except for 70% formic acid (7), in order to extract other coaggregated proteins of interest, we chose 2% SDS among several tested extraction conditions because this buffer led to the best yield of total proteins. As is well known, SDS dissolves Aβ fibrils poorly (7), and accordingly, we identified only weak Aβ immunoreactivity in the SDS-solubilized plaque sample but not in the non-plaque control by Western blotting (data not shown). However, the small amount of Aβ warranted strong signals in the LC-MS/MS analysis, which strongly suggested that many other major protein aggregates in the plaques could barely elude detection.

One major concern with this type of analysis is the purity of the plaque sample, because LC-MS/MS can detect protein species with high sensitivity. We used the LCM approach for the isolation of amyloid plaques from postmortem tissues stained by thioflavin-S. This dye preferentially labels proteins with β-sheet structures that are highly enriched in senile plaques. Under the fluorescence microscope, it is easy to distinguish senile plaques from the surrounding neuropil and from other labeled structures such as neurofibrillary tangles and amyloid deposits in blood vessels (amyloid angiopathy); and subsequent physical capture of the observed plaques individually renders highly pure preparations. Because senile plaques themselves are heterogeneous structures that may vary in their protein composition, one important question is whether the proteins identified are present in all senile plaques or whether the diversity is contributed by heterogeneous senile plaques.

Among the two phosphorylated peptides identified in neurofilament 3 (medium chain), one peptide displays the repeated KSPV motif that is homologous to neurofilament heavy chain and tau (70). Hyperphosphorylation of neurofilament as well as tau may lead to abnormal microtubule network assembly and disruption of vesicle transport (71, 72), potentially resulting in neuritic degeneration around the pathological plaque structure. We failed to find with confidence phosphopeptides derived from other proteins such as tau, because in the LC-MS/MS analysis, only peptides with strong signals were selected for sequencing; thus, the majority of peptides generated from a complex mixture was missed by the mass spectrometer. To gain a more complete view of the phosphorylation events in the plaques, specific enrichment of the modified forms of proteins/peptides will be required.

The combination of laser capture microdissection with LC-MS/MS provides a general method integrating a cellular staining approach with biochemical protein analysis, which permits the direct sequencing of proteins present in a specific microscopic region with high sensitivity, as evidenced by the identification of several hundreds of proteins from less than 5 μg of total plaque proteins. By applying different staining methods that specifically label other types of plaques such as diffuse and primitive plaques, this methodology can be further extended to determine proteins involved in the early stages of aggregation and possibly illustrate the molecular events that initiate the plaque formation. This approach can also be applied to study plaque evolution in the transgenic mouse model. Furthermore, it is possible to use this technology for the analysis of other pathological structures such as Lewy bodies in Parkinson's disease, protein inclusions in Huntington's disease, or ubiquitin-positive inclusions in frontotemporal dementia. On the other hand, the LC-MS/MS approach itself has been used as a primary tool to allow highly sensitive protein identification and to provide protein quantification information by integrating the extracted ion current of eluted peptides. More accurate quantification of proteins could be achieved by applying stable isotope labeling based techniques such as isotope-coded affinity tag strategy (73).

To our knowledge, this is the first large scale analysis of proteins from AD amyloid plaques. The results of this study demonstrate that the protein molecules in amyloid plaques are highly complex and diverse, implicating the involvement of many cellular pathways in disease development. The plaque subproteome identified in our study will be instructive for subsequent hypothesis-driven experiments on disease biomarker identification and molecular genesis of Alzheimer's disease.

Acknowledgments—We thank Dr. Michael Iuvone and James Wessel for their help in LCM. We also thank Dr. Steven Gygi, Carson Thoreen, and Rob Duarte for their help in computational analysis; Stephanie Carter for maintaining the animals; Sara Dodson for making mouse brain sections. In addition, we are grateful to Drs. Victor Faundez, John Wood, and Deanna Smith for providing antibodies.

REFERENCES

1. Hardy, J., and Selkoe, D. J. (2002) *Science* **297,** 353–356
2. Lee, V. M., Goedert, M., and Trojanowski, J. Q. (2001) *Annu. Rev. Neurosci.* **24,** 1121–1159
3. Blass, J. P. (2001) *J. Neurosci. Res.* **66,** 851–856
4. Nunomura, A., Perry, G., Aliev, G., Hirai, K., Takeda, A., Balraj, E. K., Jones, P. K., Ghanbari, H., Wataya, T., Shimohama, S., Chiba, S., Atwood, C. S., Petersen, R. B., and Smith, M. A. (2001) *J. Neuropathol. Exp. Neurol.* **60,** 759–767
5. Akiyama, H., Barger, S., Barnum, S., Bradt, B., Bauer, J., Cole, G. M., Cooper, N. R., Eikelenboom, P., Emmerling, M., Fiebich, B. L., Finch, C. E., Frautschy, S., Griffin, W. S., Hampel, H., Hull, M., Landreth, G., Lue, L., Mrak, R., Mackenzie, I. R., McGeer, P. L., O'Banion, M. K., Pachter, J., Pasinetti, G., Plata-Salaman, C., Rogers, J., Rydel, R., Shen, Y., Streit, W., Strohmeyer, R., Tooyoma, I., Van Muiswinkel, F. L., Veerhuis, R., Walker, D., Webster, S., Wegrzyniak, B., Wenk, G., and Wyss-Coray, T. (2000) *Neurobiol. Aging* **21,** 383–421
6. Glenner, G. G., and Wong, C. W. (1984) *Biochem. Biophys. Res. Commun.* **120,** 885–890
7. Masters, C. L., Simms, G., Weinman, N. A., Multhaup, G., McDonald, B. L., and Beyreuther, K. (1985) *Proc. Natl. Acad. Sci. U. S. A.* **82,** 4245–4249
8. Terry, R. D., Gonatas, N. K., and Weiss, M. (1964) *Am. J. Pathol.* **44,** 269–297
9. Butterfield, D. A., Boyd-Kimball, D., and Castegna, A. (2003) *J. Neurochem.* **86,** 1313–1327
10. Tsuji, T., Shiozaki, A., Kohno, R., Yoshizato, K., and Shimohama, S. (2002) *Neurochem. Res.* **27,** 1245–1253
11. Schonberger, S. J., Edgar, P. F., Kydd, R., Faull, R. L., and Cooper, G. J. (2001) *Proteomics* **1,** 1519–1528
12. Aebersold, R., and Mann, M. (2003) *Nature* **422,** 198–207
13. Washburn, M. P., Wolters, D., and Yates, J. R., III (2001) *Nat. Biotechnol.* **19,** 242–247
14. Andersen, J. S., Lyon, C. E., Fox, A. H., Leung, A. K., Lam, Y. W., Steen, H., Mann, M., and Lamond, A. I. (2002) *Curr. Biol.* **12,** 1–11
15. Andersen, J. S., Wilkinson, C. J., Mayor, T., Mortensen, P., Nigg, E. A., and Mann, M. (2003) *Nature* **426,** 570–574
16. Schirmer, E. C., Florens, L., Guan, T., Yates, J. R., III, and Gerace, L. (2003) *Science* **301,** 1380–1382
17. Mootha, V. K., Bunkenborg, J., Olsen, J. V., Hjerrild, M., Wisniewski, J. R., Stahl, E., Bolouri, M. S., Ray, H. N., Sihag, S., Kamal, M., Patterson, N., Lander, E. S., and Mann, M. (2003) *Cell* **115,** 629–640
18. Peng, J., Kim, M. J., Cheng, D., Duong, D. M., Gygi, S. P., and Sheng, M. (2004) *J. Biol. Chem.* **279,** 21003–21011
19. Blagoev, B., Kratchmarova, I., Ong, S. E., Nielsen, M., Foster, L. J., and Mann, M. (2003) *Nat. Biotechnol.* **21,** 315–318
20. Shiio, Y., Donohoe, S., Yi, E. C., Goodlett, D. R., Aebersold, R., and Eisenman, R. N. (2002) *EMBO J.* **21,** 5088–5096
21. Mann, M., and Jensen, O. N. (2003) *Nat. Biotechnol.* **21,** 255–261
22. Peng, J., Schwartz, D., Elias, J. E., Thoreen, C. C., Cheng, D., Marsischky, G., Roelofs, J., Finley, D., and Gygi, S. P. (2003) *Nat. Biotechnol.* **21,** 921–926
23. Simone, N. L., Bonner, R. F., Gillespie, J. W., Emmert-Buck, M. R., and Liotta, L. A. (1998) *Trends Genet.* **14,** 272–276
24. Zhou, G., Li, H., DeCamp, D., Chen, S., Shu, H., Gong, Y., Flaig, M., Gillespie, J. W., Hu, N., Taylor, P. R., Emmert-Buck, M. R., Liotta, L. A., Petricoin, E. F., III, and Zhao, Y. (2002) *Mol. Cell. Proteomics* **1,** 117–124
25. Jones, M. B., Krutzsch, H., Shu, H., Zhao, Y., Liotta, L. A., Kohn, E. C., and Petricoin, E. F., III (2002) *Proteomics* **2,** 76–84
26. Mirra, S. S., Heyman, A., McKeel, D., Sumi, S. M., Crain, B. J., Brownlee, L. M., Vogel, F. S., Hughes, J. P., van Belle, G., and Berg, L. (1991) *Neurology* **41,** 479–486
27. Emmert-Buck, M. R., Bonner, R. F., Smith, P. D., Chuaqui, R. F., Zhuang, Z., Goldstein, S. R., Weiss, R. A., and Liotta, L. A. (1996) *Science* **274,** 998–1001
28. Shevchenko, A., Wilm, M., Vorm, O., and Mann, M. (1996) *Anal. Chem.* **68,** 850–858
29. Peng, J., and Gygi, S. P. (2001) *J. Mass Spectrom.* **36,** 1083–1091
30. Eng, J., McCormack, A. L., and Yates, J. R., III (1994) *J. Am. Soc. Mass Spectrom.* **5,** 976–989

31. Link, A. J., Eng, J., Schieltz, D. M., Carmack, E., Mize, G. J., Morris, D. R., Garvik, B. M., and Yates, J. R., III (1999) *Nat. Biotechnol.* **17,** 676–682
32. Peng, J., Elias, J. E., Thoreen, C. C., Licklider, L. J., and Gygi, S. P. (2003) *J. Proteome Res.* **2,** 43–50
33. Rappsilber, J., and Mann, M. (2002) *Trends Biochem. Sci.* **27,** 74–78
34. Wang, W., Zhou, H., Lin, H., Roy, S., Shaler, T. A., Hill, L. R., Norton, S., Kumar, P., Anderle, M., and Becker, C. H. (2003) *Anal. Chem.* **75,** 4818–4826
35. Chelius, D., Zhang, T., Wang, G., and Shen, R. F. (2003) *Anal. Chem.* **75,** 6658–6665
36. Borchelt, D. R., Ratovitski, T., van Lare, J., Lee, M. K., Gonzales, V., Jenkins, N. A., Copeland, N. G., Price, D. L., and Sisodia, S. S. (1997) *Neuron* **19,** 939–945
37. Wong, P. C., Cai, H., Borchelt, D. R., and Price, D. L. (2002) *Nat. Neurosci.* **5,** 633–639
38. Sanders, S. L., Jennings, J., Canutescu, A., Link, A. J., and Weil, P. A. (2002) *Mol. Cell. Biol.* **22,** 4723–4738
39. Rappsilber, J., Ryder, U., Lamond, A. I., and Mann, M. (2002) *Genome Res.* **12,** 1231–1245
40. Atwood, C. S., Martins, R. N., Smith, M. A., and Perry, G. (2002) *Peptides* **23,** 1343–1350
41. Terry, R. D. (1998) *J. Neural Transm.* **53,** (suppl.) 141–145
42. Kinoshita, A., Kinoshita, M., Akiyama, H., Tomimoto, H., Akiguchi, I., Kumar, S., Noda, M., and Kimura, J. (1998) *Am. J. Pathol.* **153,** 1551–1560
43. Mandybur, T. I., and Chuirazzi, C. C. (1990) *Neurology* **40,** 635–639
44. Meda, L., Baron, P., and Scarlato, G. (2001) *Neurobiol. Aging* **22,** 885–893
45. Renkawek, K., Bosman, G. J., and Gaestel, M. (1993) *Neuroreport* **5,** 14–16
46. Layfield, R., Fergusson, J., Aitken, A., Lowe, J., Landon, M., and Mayer, R. J. (1996) *Neurosci. Lett.* **209,** 57–60
47. Hashiguchi, M., Sobue, K., and Paudel, H. K. (2000) *J. Biol. Chem.* **275,** 25247–25254
48. Hu, Y. Y., He, S. S., Wang, X. C., Duan, Q. H., Khatoon, S., Iqbal, K., Grundke-Iqbal, I., and Wang, J. Z. (2002) *Neurosci. Lett.* **320,** 156–160
49. Forloni, G., Terreni, L., Bertani, I., Fogliarino, S., Invernizzi, R., Assini, A., Ribizzi, G., Negro, A., Calabrese, E., Volonte, M. A., Mariani, C., Franceschi, M., Tabaton, M., and Bertoli, A. (2002) *Neurobiol. Aging* **23,** 957–976
50. Levy, E., Sastre, M., Kumar, A., Gallo, G., Piccardo, P., Ghetti, B., and Tagliavini, F. (2001) *J. Neuropathol. Exp. Neurol.* **60,** 94–104
51. Deng, A., Irizarry, M. C., Nitsch, R. M., Growdon, J. H., and Rebeck, G. W. (2001) *Am. J. Pathol.* **159,** 1061–1068
52. Crawford, F. C., Freeman, M. J., Schinka, J. A., Abdullah, L. I., Gold, M., Hartman, R., Krivian, K., Morris, M. D., Richards, D., Duara, R., Anand, R., and Mullan, M. J. (2000) *Neurology* **55,** 763–768
53. Breitner, J. C. (1996) *Neurobiol. Aging* **17,** 789–794
54. Combs, C. K., Johnson, D. E., Karlo, J. C., Cannady, S. B., and Landreth, G. E. (2000) *J. Neurosci.* **20,** 558–567
55. Hafezparast, M., Klocke, R., Ruhrberg, C., Marquardt, A., Ahmad-Annuar, A., Bowen, S., Lalli, G., Witherden, A. S., Hummerich, H., Nicholson, S., Morgan, P. J., Oozageer, R., Priestley, J. V., Averill, S., King, V. R., Ball, S., Peters, J., Toda, T., Yamamoto, A., Hiraoka, Y., Augustin, M., Korthaus, D., Wattler, S., Wabnitz, P., Dickneite, C., Lampel, S., Boehme, F., Peraus, G., Popp, A., Rudelius, M., Schlegel, J., Fuchs, H., Hrabe de Angelis, M., Schiavo, G., Shima, D. T., Russ, A. P., Stumm, G., Martin, J. E., and Fisher, E. M. (2003) *Science* **300,** 808–812
56. Kopec, K., and Chambers, J. P. (1997) *Proc. Soc. Exp. Biol. Med.* **216,** 429–437
57. Ahmad, F. J., Echeverri, C. J., Vallee, R. B., and Baas, P. W. (1998) *J. Cell Biol.* **140,** 391–401
58. Abraham, C. R., Selkoe, D. J., and Potter, H. (1988) *Cell* **52,** 487–501
59. Namba, Y., Tomonaga, M., Kawasaki, H., Otomo, E., and Ikeda, K. (1991) *Brain Res.* **541,** 163–166
60. Hashimoto, T., Wakabayashi, T., Watanabe, A., Kowa, H., Hosoda, R., Nakamura, A., Kanazawa, I., Arai, T., Takio, K., Mann, D. M., and Iwatsubo, T. (2002) *EMBO J.* **21,** 1524–1534
61. Vinters, H. V., Nishimura, G. S., Secor, D. L., and Pardridge, W. M. (1990) *Am. J. Pathol.* **137,** 233–240
62. Masliah, E., Iwai, A., Mallory, M., Ueda, K., and Saitoh, T. (1996) *Am. J. Pathol.* **148,** 201–210
63. Snow, A. D., Mar, H., Nochlin, D., Kimata, K., Kato, M., Suzuki, S., Hassell, J., and Wight, T. N. (1988) *Am. J. Pathol.* **133,** 456–463
64. May, P. C., Lampert-Etchells, M., Johnson, S. A., Poirier, J., Masters, J. N., and Finch, C. E. (1990) *Neuron* **5,** 831–839
65. Narita, M., Holtzman, D. M., Schwartz, A. L., and Bu, G. (1997) *J. Neurochem.* **69,** 1904–1911
66. Furuta, A., Price, D. L., Pardo, C. A., Troncoso, J. C., Xu, Z. S., Taniguchi, N., and Martin, L. J. (1995) *Am. J. Pathol.* **146,** 357–367
67. Smith, M. A., Kutty, R. K., Richey, P. L., Yan, S. D., Stern, D., Chader, G. J., Wiggert, B., Petersen, R. B., and Perry, G. (1994) *Am. J. Pathol.* **145,** 42–47
68. Pappolla, M. A., Omar, R. A., Kim, K. S., and Robakis, N. K. (1992) *Am. J. Pathol.* **140,** 621–628
69. Kalaria, R. N., Kroon, S. N., Grahovac, I., and Perry, G. (1992) *Neuroscience* **51,** 177–184
70. Lichtenberg-Kraag, B., Mandelkow, E. M., Biernat, J., Steiner, B., Schroter, C., Gustke, N., Meyer, H. E., and Mandelkow, E. (1992) *Proc. Natl. Acad. Sci. U. S. A.* **89,** 5384–5388
71. Ahlijanian, M. K., Barrezueta, N. X., Williams, R. D., Jakowski, A., Kowsz, K. P., McCarthy, S., Coskran, T., Carlo, A., Seymour, P. A., Burkhardt, J. E., Nelson, R. B., and McNeish, J. D. (2000) *Proc. Natl. Acad. Sci. U. S. A.* **97,** 2910–2915
72. Trinczek, B., Ebneth, A., Mandelkow, E. M., and Mandelkow, E. (1999) *J. Cell Sci.* **112,** 2355–2367
73. Gygi, S. P., Rist, B., Gerber, S. A., Turecek, F., Gelb, M. H., and Aebersold, R. (1999) *Nat. Biotechnol.* **17,** 994–999